Journal of Power Sources 196 (2011) 6735–6741

Contents lists available at ScienceDirect

Journal of Power Sources

journal homepage: www.elsevier.com/locate/jpowsour

All-solid-state lithium secondary batteries using $LiCoO_2$ particles with pulsed laser deposition coatings of Li_2S–P_2S_5 solid electrolytes

Atsushi Sakuda[a], Akitoshi Hayashi[a], Takamasa Ohtomo[b], Shigenori Hama[b], Masahiro Tatsumisago[a,*]

[a] Department of Applied Chemistry, Graduate School of Engineering, Osaka Prefecture University, 1-1, Gakuen-cho, Naka-ku, Sakai, Osaka 599-8531, Japan
[b] Battery Research Div., Toyota Motor Corporation, Higashifuji Technical Center, 1200, Mishuku, Susono, Shizuoka 410-1193, Japan

ARTICLE INFO

Article history:
Received 23 August 2010
Received in revised form 12 October 2010
Accepted 29 October 2010
Available online 9 November 2010

Keywords:
Lithium battery
All-solid-state battery
Thin film
Sulfide electrolyte
Pulsed laser deposition
Surface coating

ABSTRACT

Electrode–electrolyte composite materials were prepared by coating a highly conductive Li_2S–P_2S_5 solid electrolyte onto $LiCoO_2$ electrode particles using pulsed laser deposition (PLD). Cross-sections of the composite electrode layers of the all-solid-state cells were observed using a transmission electron microscope to investigate the packing morphology of the $LiCoO_2$ particles and the distribution of solid electrolyte in the composite electrode. All-solid-state cells based on a composite electrode composed entirely of solid-electrolyte-coated $LiCoO_2$ were fabricated, and their performance was investigated. The coating amounts of Li_2S–P_2S_5 solid electrolytes on $LiCoO_2$ particles and the conductivity of the coating material were controlled to increase the capacity of the resulting all-solid-state cells. All-solid-state cells using $LiCoO_2$ with thick solid electrolyte coatings, grown over 120 min, had a capacity of 65 mAh g^{-1}, without any addition of Li_2S–P_2S_5 solid electrolyte particles to the composite electrode. The capacity of the all-solid-state cell increased further after increasing the conductivity of the Li_2S–P_2S_5 solid electrolyte coating by heat treatment at 200 °C. Furthermore, an all-solid-state cell based on a composite electrode using both a solid electrolyte coating and added solid electrolyte particles was fabricated, and the capacity of the resulting all-solid-state cell increased to 95 mAh g^{-1}.

1. Introduction

Lithium-ion secondary batteries are capable of a high energy density, high power, and long cycle performance [1]. Demand for lithium-ion secondary batteries has increased for applications ranging from portable devices to large machines such as electric vehicles and high-power tools. Large machines typically require much larger batteries than portable devices do. Lithium-ion secondary batteries using ionic liquid electrolytes [2–5] and solid electrolytes using organic polymers [6,7], inorganic crystals [8–11], glasses [12,13], and glass ceramics [14–17] have been studied, because the batteries are expected to be safer and more reliable. In particular, all-solid-state lithium secondary batteries using inorganic solid electrolytes have been studied as promising next-generation batteries. Because of the use of inorganic solid electrolytes instead of organic liquid electrolytes, these batteries have many advantages, such as higher safety, no leakage, a long charge–discharge life [14,17], a wide operation temperature range [18], and the potential application of new electrode materials that are difficult to use in conventional batteries.

It is important to use solid electrolytes with high lithium-ion conductivity in the development of all-solid-state batteries with high energy and power densities. Sulfide-based solid electrolytes such as thio-LISICON ($Li_{3.25}Ge_{0.25}P_{0.75}S_4$) crystals and Li_2S–P_2S_5 glass-ceramics have a high lithium-ion conductivity of over 10^{-3} S cm^{-1} at room temperature [19–21]. The lithium-ion conductivity of solid electrolytes has improved year by year, and has reached values approaching 10^{-2} S cm^{-1}. Furthermore, these solid electrolytes have an ideal transference number ($t = \sigma_{Li}/\sigma_{total}$) of almost 1 [22].

One disadvantage of all-solid-state batteries is the difficulty of forming an effective electrode–electrolyte interface. Designing a favorable composite electrode is important to the development of all-solid-state batteries. In all-solid-state battery systems using sulfide-based solid electrolytes, high interfacial resistances between the positive electrode and the solid electrolyte have been observed after the initial charging process when $LiCoO_2$ was used as the electrode active material [9,10,18,23–26]. We believe that the high resistance was caused by degradation of the interface between the $LiCoO_2$ and the Li_2S–P_2S_5 solid electrolyte [18]. Forming a favorable electrode/electrolyte interface by interfacial modification has effectively decreased the interfacial resistance. Coatings of oxides such as $Li_4Ti_5O_{12}$, $LiNbO_3$, $LiTaO_3$, Li_2O–SiO_2, and Li_2O–TiO_2 on $LiCoO_2$ particles have been reported as an effective modification technique [9,10,18,23–26]. The formation of effective electron

* Corresponding author. Tel.: +81 72 254 9331; fax: +81 72 254 9331.
E-mail address: tatsu@chem.osakafu-u.ac.jp (M. Tatsumisago).

0378-7753/$ – see front matter © 2010 Elsevier B.V. All rights reserved.
doi:10.1016/j.jpowsour.2010.10.103

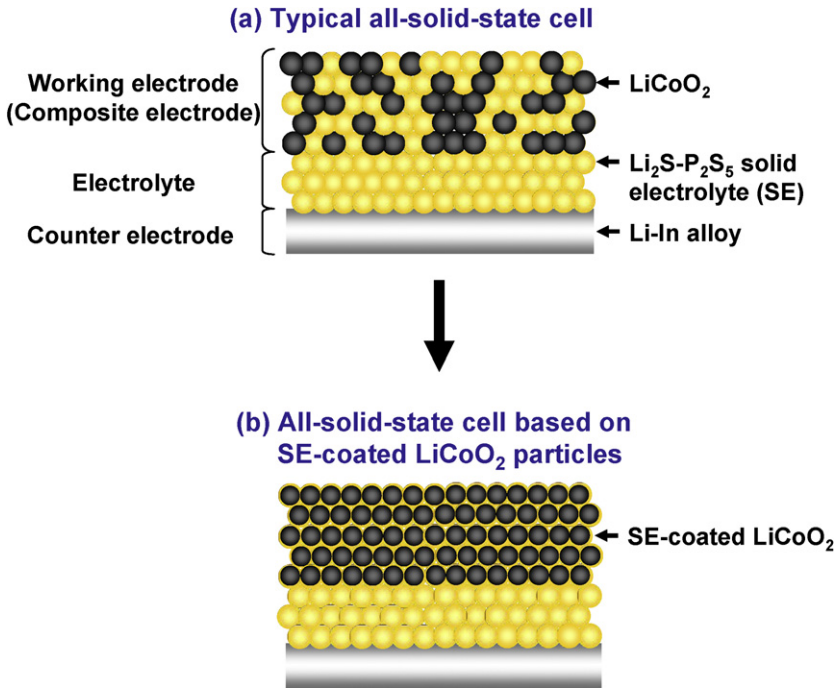

Fig. 1. Schematic diagrams of (a) a typical all-solid-state cell and (b) an all-solid-state cell based on SE-coated $LiCoO_2$ particles.

and lithium-ion conducting paths to the electrode active materials is also important. Fig. 1 shows schematic diagrams of typical bulk-type all-solid-state cells (a) and all-solid-state cells using solid-electrolyte-coated $LiCoO_2$ (SE-coated $LiCoO_2$) (b). In typical all-solid-state cells, a composite electrode composed of $LiCoO_2$ electrode particles and Li_2S–P_2S_5 solid electrolyte particles is used as a working electrode to provide a lithium ion conducting path to the $LiCoO_2$. The amount of solid electrolyte particles needed in the composite electrode is currently approximately 20–30 wt.% [27]. In addition, electron conducting additives such as acetylene black (AB) and vapor grown carbon fiber (VGCF) are required when using electrode active materials with a low electron conductivity. A decrease in solid electrolyte content combined with the use of a conducting additive can effectively increase the energy density of a composite electrode. Recently, we reported that a highly conductive Li_2S–P_2S_5 solid electrolyte was coated on $LiCoO_2$ particles using pulsed laser deposition (PLD) [28]. A schematic diagram of an all-solid-state cell using SE-coated $LiCoO_2$ is shown in Fig. 1(b). In the all-solid-state cells using SE-coated $LiCoO_2$, favorable contact between the $LiCoO_2$ electrode and the Li_2S–P_2S_5 solid electrolytes may be possible. In addition, the solid electrolyte content of the composite electrode would be reduced significantly. In the previous study [28], an all-solid-state cell based on SE-coated $LiCoO_2$ was successfully charged and discharged, indicating that the coated solid electrolyte acted as a lithium ion conducting path to the electrode particles. However, the reversible capacity of the all-solid-state cells was limited to 30 mAh g^{-1}, and this low cell capacity required improvement. The conductivity of an Li_2S–P_2S_5 solid electrolyte film prepared on a quartz substrate by PLD was reported to increase after heat treatment at 200 °C [29]. The conductivity of an Li_2S–P_2S_5 solid electrolyte on $LiCoO_2$ should therefore also increase with heat treatment.

In this study, we fabricated all-solid-state cells based on a composite electrode composed of SE-coated $LiCoO_2$, and examined the amount and conductivity of an SE coating on the $LiCoO_2$. The effect of the coating amount on the capacity was investigated by preparing all-solid-state cells with SE-coated $LiCoO_2$ using various SE coating times. The importance of the lithium ion conductivity of the coating layer was studied by increasing the lithium ion conductivity of the SE on the $LiCoO_2$ particles by heat treatment at 200 °C. Cross-sections of the composite electrodes in the all-solid-state cells were observed using a transmission electron microscope (TEM) to investigate the packing morphology of the SE-coated $LiCoO_2$ particles and the elemental distribution at the interfaces between the particles. Moreover, all-solid-state cells based on composite electrodes using both a solid electrolyte coating and added solid electrolyte particles were fabricated in an attempt to improve the capacity of the cells.

2. Experimental

An $80Li_2S{\cdot}20P_2S_5$ solid electrolyte (SE) was coated on $LiCoO_2$ particles using pulsed laser deposition (PLD). SE thin films of $80Li_2S{\cdot}20P_2S_5$ (mol.%) SE were fabricated using PLD with a KrF excimer laser (λ = 248 nm, LPXPro, Lambda Physik) [29]. The deposition conditions are summarized in Table 1. A pelletized mixture of Li_2S (99.9%; Idemitsu Kosan Co., Ltd.) and P_2S_5 crystalline powder (99%, Aldrich Chemical Co. Inc.) with a molar ratio of 80:20 was used as a target. The $80Li_2S{\cdot}20P_2S_5$ films deposited on Si substrates were amorphous. The atomic ratio of Li:P in the film was determined by inductively coupled plasma atomic emission spectroscopy (ICP-AES) to be 80:20, which corresponds to the Li:P ratio of the target. The lithium ion conductivity of the $80Li_2S{\cdot}20P_2S_5$ was 7.9×10^{-5} S cm^{-1} at 25 °C [29]. An $80Li_2S{\cdot}20P_2S_5$ SE film was

Table 1
Deposition condition of Li_2S–P_2S_5 solid electrolyte film.

Laser	KrF excimer laser (248 nm)
Target	Li_2S:P_2S_5 = 80:20 (molar ratio)
Laser fluence	ca. 2 J cm^{-2} (200 mJ per pulse)
Frequency	10 Hz
Temperature	Room temperature
Ambient gas	Ar gas
Gas pressure	5 Pa
Deposition time	10 min, 20 min, 40 min, 120 min
T–S distance (target–substrate distance)	7 cm

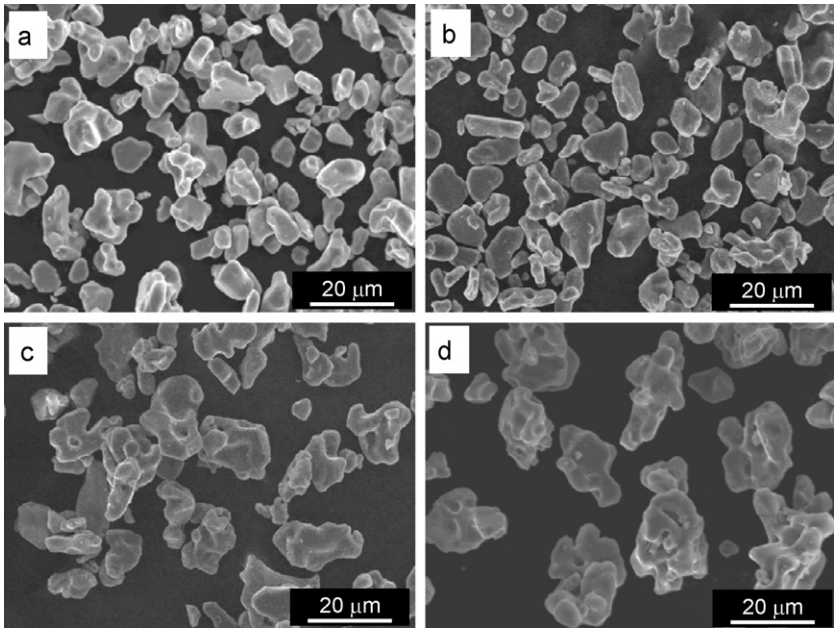

Fig. 2. SEM images of SE-coated $LiCoO_2$ with various coating times: (a) 0 min, (b) 10 min, (c) 20 min, and (d) 40 min.

deposited on $LiCoO_2$ particles (D-10, Toda Kogyo Corp.) [28]. In this study, the $LiCoO_2$ particles for all the SE-coated $LiCoO_2$ were coated with an $LiNbO_3$ film in advance, because $LiNbO_3$-coated $LiCoO_2$ has demonstrated good rate performance in all-solid-state batteries using a sulfide-based SE [10]. Target holders were attached to the upper side of the PLD vacuum chamber, and a vibrating sample holder was equipped at the lower side. This PLD system allowed the formation of an SE layer on the electrode particles. During deposition of the SE, $LiCoO_2$ particles were fluidized by a vibration system (VIB-FB, Nara Machinery Co., Ltd.) to form a uniform SE layer on the $LiCoO_2$ particles. The frequency of the square pulse used to fluidize the particles was 50 Hz. The deposition time was varied from 0 min to 120 min to obtain Li_2S–P_2S_5 coatings of different thicknesses. Heat treatment of SE-coated $LiCoO_2$ was performed in an Ar atmosphere. In order to avoid exposure to air, an Ar-filled glove box was connected to the vacuum chamber for deposition. The morphology of the $LiCoO_2$ particles was observed using a scanning electron microscope (SEM, Tiny SEM Mighty-8; Technex Lab. Co., Ltd).

All-solid-state cells (In/$80Li_2S{\cdot}20P_2S_5$ glass-ceramic SE/$LiCoO_2$) were constructed to investigate the electrochemical performance of $LiCoO_2$ coated with $80Li_2S{\cdot}20P_2S_5$ SE. Preparation of the $80Li_2S{\cdot}20P_2S_5$ glass-ceramic SE particles and the fabrication of all-solid-state cells were described in our previous reports [9,10,18,24–26]. Indium foil (99.999%; Furuuchi Chemical Corp.) was used as a counter electrode. Li_2S–P_2S_5 SE particles were added to the working electrode layer in the previous reports, in which the working electrode consisted of 70 wt.% $LiCoO_2$ particles and 30 wt.% Li_2S–P_2S_5 glass ceramic SE particles. In this study, SE particles were not added to the working layer of some electrodes, so that the effect of the SE coating on the $LiCoO_2$ particles could be investigated. The resulting working electrodes consisted of only SE-coated $LiCoO_2$ particles. Other working electrodes, consisting of 90 wt.% SE-coated $LiCoO_2$ particles and 10 wt.% Li_2S–P_2S_5 SE particles, were also prepared. As a result of the mixing, these electrodes had a lower SE particle content. A bilayer pellet consisting of a working electrode (10 mg) and a glass-ceramic SE (80 mg) was obtained by pressing at 360 MPa (ϕ = 10 mm). Then, an indium foil was attached to the bilayer pellet by pressing at 240 MPa. The pellet was pressed using two stainless steel rods, which were used as current collectors for the working and counter electrodes.

The all-solid-state cells were charged and discharged using a charge–discharge measuring device (BTS-2004; Nagano Co., Ltd.) at room temperature. Electrochemical impedance spectroscopy measurements of the all-solid-state cells were performed using an impedance analyzer (SI 1260; Solartron) after charging the cells to 3.6 V vs. Li–In at 0.13 mA cm^{-2} at room temperature. The applied voltage was 50 mV, and the frequency ranged from 1 Hz to 1 MHz. The interfaces between $LiCoO_2$ particles coated with the $80Li_2S{\cdot}20P_2S_5$ film in the working electrode were observed using a transmission electron microscope (TEM, JEM2100F; JEOL) to investigate the morphology of the coating between $LiCoO_2$ particles. Samples for TEM observation were obtained using focused ion beam (FIB) milling. The samples were transferred in an Ar atmosphere from the glove box to the FIB and TEM equipment.

3. Results and discussion

$80Li_2S{\cdot}20P_2S_5$ SE was coated on $LiCoO_2$ particles by PLD. Fig. 2 shows SEM images of $80Li_2S{\cdot}20P_2S_5$ SE coated $LiCoO_2$ (SE-coated $LiCoO_2$) with different coating times, ranging from 0 to 40 min. Fig. 2(a) shows an SEM image of $LiNbO_3$-coated $LiCoO_2$ without an Li_2S–P_2S_5 SE coating. The average particle diameter was ca. 10 μm, and the surface of the $LiNbO_3$-coated $LiCoO_2$ particles was relatively smooth. The particle size of the SE (10 min)-coated $LiCoO_2$, as shown in Fig. 2(b), was similar to that without SE coating. Fig. 2(c) and (d) shows SEM images of SE (20 min)-coated and SE (40 min)-coated $LiCoO_2$. The particle sizes of the 20-min and 40-min SE-coated $LiCoO_2$ were ca. 20 μm, which was larger than that without SE coating. Small aggregates were formed by depositing Li_2S–P_2S_5 SE on $LiCoO_2$ particles, and the size of the secondary particles increased with increasing deposition time. The SE coating on the $LiCoO_2$ particles was confirmed using EDX mapping images and cross-sectional TEM images in the previous report [28]. A cross-sectional TEM image of SE (40 min)-coated $LiCoO_2$ showed that the $80Li_2S{\cdot}20P_2S_5$ SE was coated on the $LiCoO_2$ particles with a thickness of ca. 50–70 nm after coating for 40 min, corresponding to ca. 1 wt.% $LiCoO_2$. SE coating for 120 min was estimated to yield about 3 wt.% $LiCoO_2$.

All-solid-state cells were constructed using SE-coated $LiCoO_2$ particles with no SE particles mixed into the working electrode. The

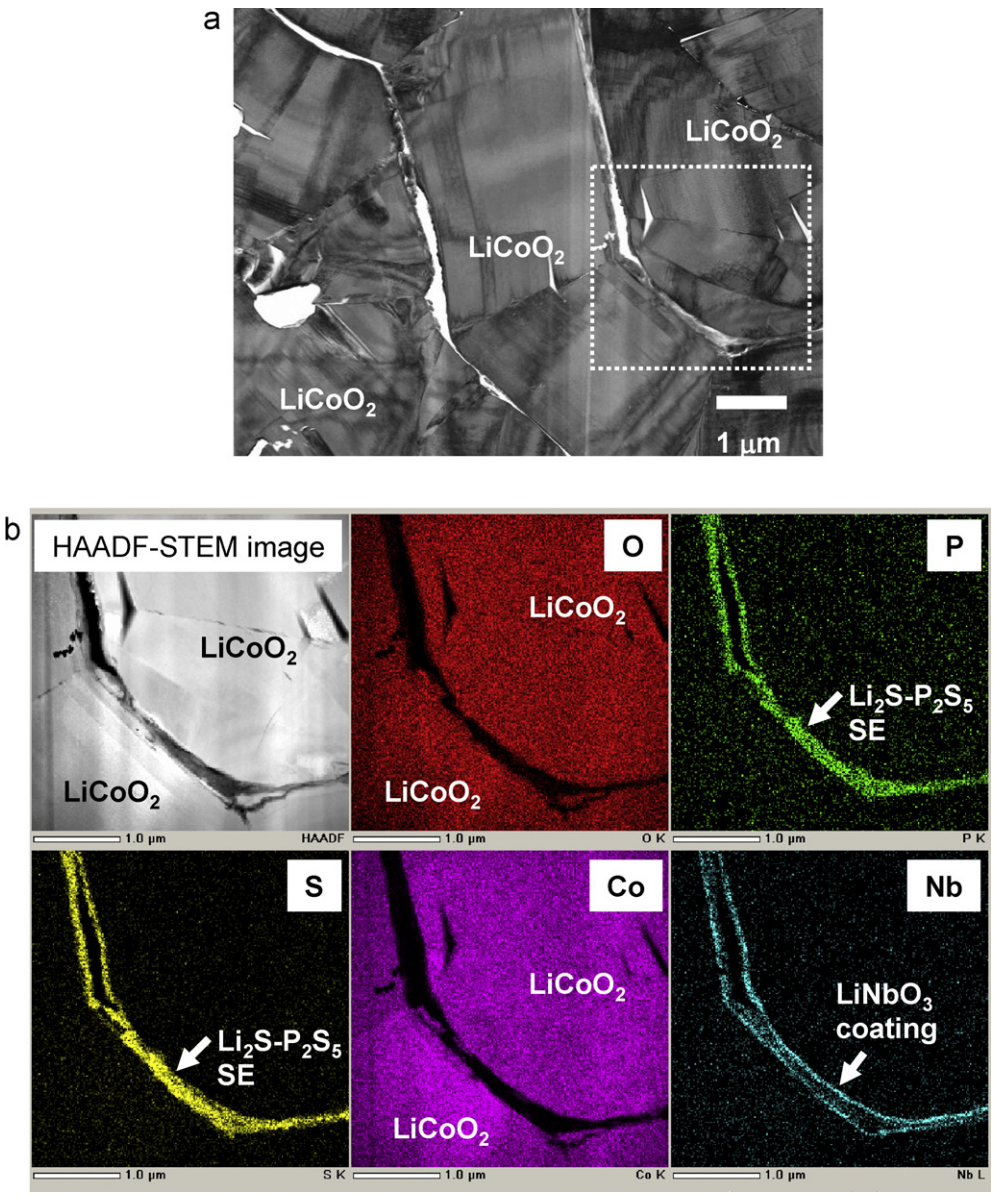

Fig. 3. Cross-sectional high-angle annular dark field (HAADF) TEM images and EDX mappings of a composite electrode composed of SE-coated $LiCoO_2$ in an all-solid-state cell after 450 cycles. The composite electrode was composed of solely SE-coated $LiCoO_2$, with no added SE particles.

all-solid-state cell using SE (40 min)-coated $LiCoO_2$ was charged and discharged with no capacity fade [28]. A cross section of the working electrode of the all-solid-state cell was observed to investigate how the $LiCoO_2$ particles were packed, and the Li_2S–P_2S_5 SE coating was observed at the interface between $LiCoO_2$ particles. Fig. 3 shows cross-sectional high-angle annular dark field (HAADF)-TEM images and EDX mappings of a working electrode from an all-solid-state cell based on SE (40 min)-coated $LiCoO_2$ with no additional SE particles added after charge–discharge measurements for 450 cycles. The cross-sectional TEM image in Fig. 3(a) shows that the $LiCoO_2$ particles were closely packed in the composite electrode. Fig. 3(b) shows a magnified image of the selected area in Fig. 3(a) and EDX mappings for O, P, S, Co, and Nb at the interface between $LiCoO_2$ particles. Nb was observed on the $LiCoO_2$ particle surfaces, confirming that an $LiNbO_3$ coating did form on the $LiCoO_2$ particles. The observation of P and S at the interface between the $LiCoO_2$ particles indicated that an $80Li_2S{\cdot}20P_2S_5$ SE layer was present. The all-solid-state cell was prepared by cold pressing. As a result of this pressing, the $LiCoO_2$ particles packed closely in the composite electrode layer and the SE coating deposited on the $LiCoO_2$ particles was connected to form the all-solid-state cell. As a result, a favorable SE region was formed in the interfacial space between the $LiCoO_2$ particles. Furthermore, the contact between the SE layer and the $LiCoO_2$ electrode was maintained after charge–discharge measurements. Retention of the electrode/electrolyte interface during charge–discharge cycling is important for capacity retention in all-solid-state batteries. Some voids at the interfaces between $LiCoO_2$ particles were observed, as shown in Fig. 3(a). This could be reduced using $LiCoO_2$ with larger amounts of SE coating. In an all-solid-state cell based on SE (120 min)-coated $LiCoO_2$ particles, the SE would be formed more effectively at the interface, because the SE coating thickness on the $LiCoO_2$ would be three times that of a composite electrode using SE (40 min)-coated $LiCoO_2$.

Fig. 4 shows charge–discharge curves of all-solid-state cells using uncoated, $LiNbO_3$-coated, and SE (x min)-coated $LiCoO_2$ particles (x = 10, 40, and 120 min) at a current density of 0.13 mA cm^{-2}. The SE coatings were applied to $LiNbO_3$-coated $LiCoO_2$ particles.

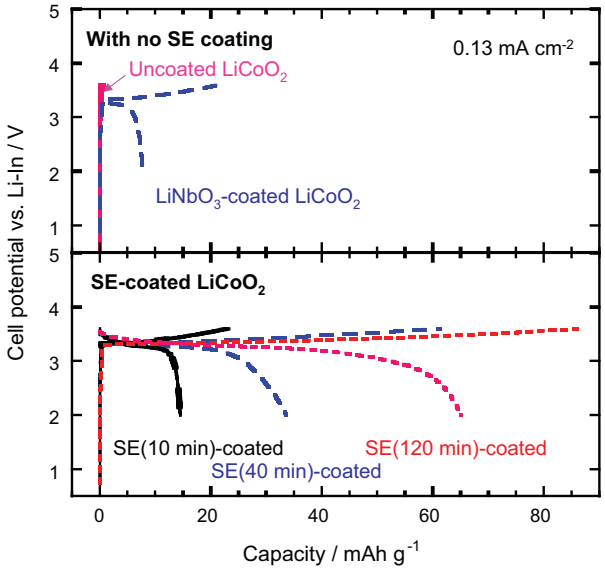

Fig. 4. Charge–discharge curves of all-solid-state cells based on non-coated, $LiNbO_3$-coated, and SE-coated $LiCoO_2$ with various coating times. The composite electrode was composed solely of coated $LiCoO_2$, with no added SE particles.

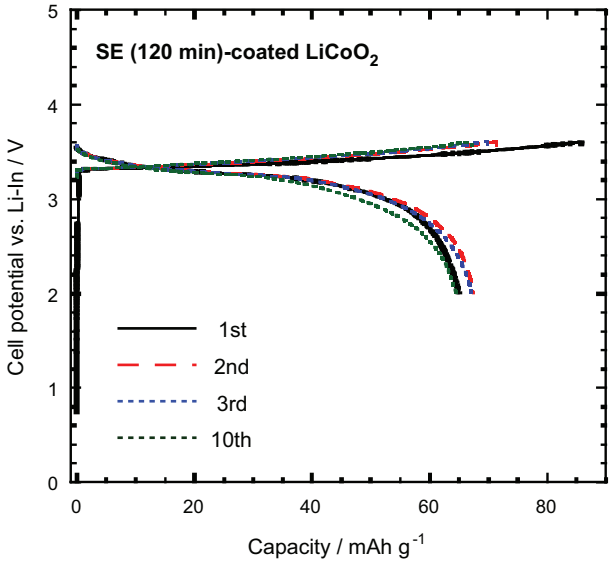

Fig. 5. Charge–discharge curves of an all-solid-state cell based on SE (120 min)-coated $LiCoO_2$.

In the all-solid-state cells shown in Fig. 4, SE particles were not mixed into the composite electrode, so the working electrode was composed of only $LiCoO_2$ particles. The displayed capacity was normalized by the weight of the coated $LiCoO_2$. The all-solid-state cell based on uncoated $LiCoO_2$ could not be charged and discharged. The all-solid-state cell using $LiNbO_3$-coated $LiCoO_2$ had a small reversible capacity of less than 10 mAh g^{-1}. All-solid-state cells using $LiCoO_2$ particles without Li_2S–P_2S_5 SE coating were difficult to charge and discharge, because the lithium ion conductivity in the composite electrolyte was insufficient. The all-solid-state cells using SE-coated $LiCoO_2$ particles could be charged and discharged with a higher capacity than $LiNbO_3$-coated $LiCoO_2$, and the all-solid-state cells using SE (10 min)-coated, SE (40 min)-coated, and SE (120 min)-coated $LiCoO_2$ had reversible capacities of 15, 35, and 65 mAh g^{-1}, respectively. In the previous study [28], only SE (40 min)-coated $LiCoO_2$ was used, and the reversible capacity of the all-solid-state cells was limited to ca. 30 mAh g^{-1}. By increasing the SE coating amount from 40 min to 120 min in this study, the capacity was increased from 35 to 65 mAh g^{-1}. The capacity increased with increasing coating time from 0 min to 120 min, which indicates that an SE coating on $LiNbO_3$-coated $LiCoO_2$ enabled the formation of a lithium-ion conducting path to the $LiCoO_2$ particles.

Fig. 5 shows the charge–discharge curves of all-solid-state cell based on SE (120 min)-coated $LiCoO_2$. The cell demonstrated stable charge and discharge curves, without a significant fade in capacity, over 10 cycles. The all-solid-state cell based on SE (40 min)-coated $LiCoO_2$ was charged and discharged for 100 cycles with no significant reduction in capacity [28].

Increasing the lithium ion conductivity in composite electrodes seems to be important in achieving a high capacity. The conductivity of the $80Li_2S{\cdot}20P_2S_5$ SE film prepared using PLD was increased by heat treatment at 200 °C [29]. Therefore, the effect of heat treatment of SE-coated $LiCoO_2$ on cell performance was investigated. Fig. 6 shows the charge–discharge curves of an all-solid-state cell based on SE (120 min)-coated $LiCoO_2$, after heat treatment at 200 °C for 1 h. The current density was 0.13 mA cm^{-2}. The charging and discharging capacities were 86 and 69 mAh g^{-1}, respectively. The charging capacities of cells based on SE (120 min)-coated $LiCoO_2$ with and without heat treatment were similar. The discharge capacity of the heat-treated SE (120 min)-coated $LiCoO_2$ cell was larger than the capacity without heat treatment. The discharge capacity increased after heat treatment of the SE-coated $LiCoO_2$. The lithium ion conductivity of the SE coated on the $LiNbO_3$-coated $LiCoO_2$ would likely be increased by heat treatment, as was observed in SE films deposited on substrates, resulting in the observed increase in capacity.

As shown above, the SE coating was effective in forming a lithium ion conducting path to the $LiCoO_2$ particles in the electrode layer. However, the capacities of these all-solid-state cells remained smaller than the 95 mAh g^{-1} typical of all-solid-state cells containing composite electrodes composed of 70 wt.% $LiNbO_3$-coated $LiCoO_2$ (with no SE coating) and 30 wt.% SE particles mixing at a current density of 0.13 mA cm^{-2}.

To increase the lithium ion conductivity in the composite electrodes, 10 wt.% SE particles were added to the SE-coated $LiCoO_2$ particles. Fig. 7 shows the impedance profiles of all-solid-state cells using composite electrodes consisting of uncoated, $LiNbO_3$-coated, or SE-coated $LiCoO_2$ with 10 wt.% SE particles. The measurements

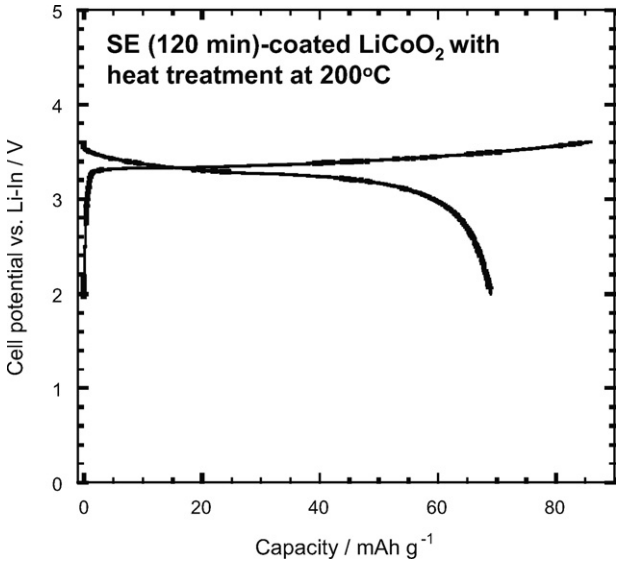

Fig. 6. Charge–discharge curves of an all-solid-state cell based on SE (120 min)-coated $LiCoO_2$ with heat treatment at 200 °C. The composite electrode was composed of SE-coated $LiCoO_2$, with no added SE particles.

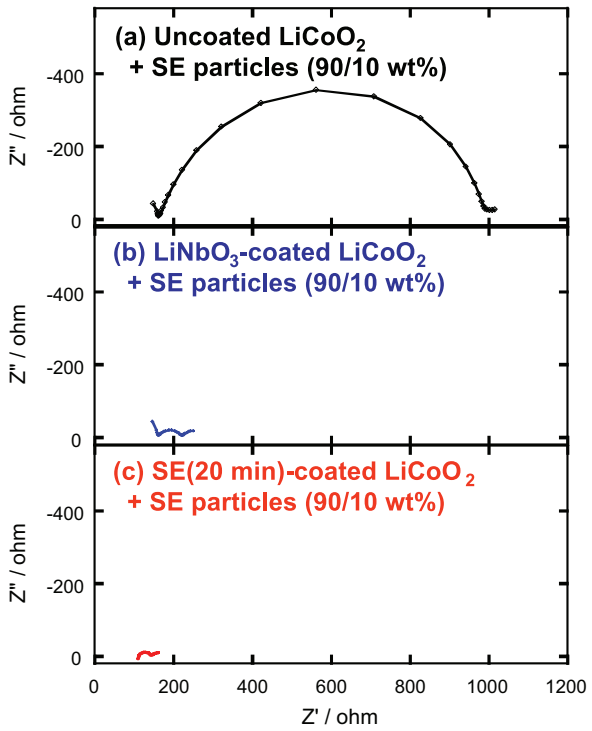

Fig. 7. Impedance profiles of all-solid-state cells based on composite electrodes with 90 wt.% $LiCoO_2$ and 10 wt.% solid electrolyte particles after charging to 3.6 V vs. Li–In. The composite electrodes were prepared using (a) uncoated $LiCoO_2$, (b) $LiNbO_3$-coated $LiCoO_2$, and (c) SE (20 min)-coated $LiCoO_2$, which was coated with $LiNbO_3$ in advance.

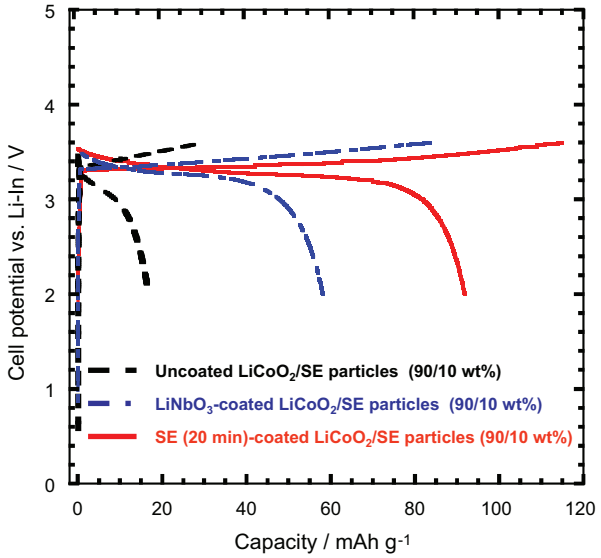

Fig. 8. Charge–discharge curves of all-solid-state cells based on composite electrodes with 90 wt.% $LiCoO_2$ and 10 wt.% solid electrolyte particles.

were carried out after charging to 3.6 V vs. a Li–In electrode, which corresponds to 4.2 V vs. Li. The large semicircle observed in panel (a) of Fig. 7 is attributable to the interfacial resistance between $LiCoO_2$ and Li_2S–P_2S_5 SE, which was reported in previous papers [9,10,25]. The interfacial resistance of the all-solid-state cell based on uncoated $LiCoO_2$ in this study was ca. 850 Ω, which was higher than our previous results of ca. 300 Ω [24–26]. This was because the contact area between the $LiCoO_2$ and the SE particles in this study was smaller than in the previous studies; only 10 wt.% SE particles were added to the $LiCoO_2$ particles in this study, whereas 30 wt.% SE particles were added in the previous studies. The all-solid-state cells based on $LiNbO_3$-coated and SE (20 min)-coated $LiCoO_2$ and shown in Fig. 7(b) and (c) had a low interfacial resistance, although only 10 wt.% SE particles were added to the $LiCoO_2$ particles. The $LiNbO_3$ coating on the $LiCoO_2$ decreased the interfacial resistance, and the additional SE (20 min) coating on the $LiCoO_2$ reduced the resistance further.

Fig. 8 shows charge–discharge curves of all-solid-state cells based on composite electrodes composed of 90 wt.% uncoated, $LiNbO_3$-coated, or SE (20 min)-coated $LiCoO_2$ and 10 wt.% SE particles, at a current density of 0.13 mA cm^{-2}. The capacities of the all-solid-state cells based on uncoated, $LiNbO_3$-coated, and SE (20 min)-coated $LiCoO_2$ particles were 20, 60, and 95 mAh g^{-1}, respectively. The capacities of the all-solid-state cells were increased using cells combining 10 wt.% SE particles and an SE coating, compared with the capacity of cells based on an SE coating alone in the composite electrode, as shown in Fig. 4. The all-solid-state cell combining 10 wt.% SE particles with an SE coating had a similar capacity to cells based on 30 wt.% SE particles with no coating.

The SE coating was effective in decreasing the SE ratio in the composite electrolyte, resulting in all-solid-state cells with an improved energy density. The energy density of the cells, normalized by the weight of the $LiCoO_2$ and Li_2S–P_2S_5 SE composite electrode, was calculated. The weight-normalized capacity of a composite containing 90 wt.% SE-coated $LiCoO_2$ and 10 wt.% SE particles, which was prepared using both an SE coating and added SE particles, was 86 mAh g^{-1}. In contrast, that of a normal composite prepared using 70 wt.% $LiNbO_3$-coated $LiCoO_2$ and 30 wt.% SE particles was 67 mAh g^{-1}. The capacity of the cells was thus increased by decreasing the amount of Li_2S–P_2S_5 SE particles in the composite electrode.

4. Conclusions

In all-solid-state cells based on SE-coated $LiCoO_2$ particles, the $LiCoO_2$ particles were closely packed in the composite electrode, and an Li_2S–P_2S_5 SE coating occupied the interface between the $LiCoO_2$ particles. All-solid-state cells containing SE-coated $LiCoO_2$ had a larger capacity than cells with no SE coating, and the charge–discharge capacity increased with increasing coating time. The heat treatment of SE-coated $LiCoO_2$ particles increased the discharge capacity. The Li_2S–P_2S_5 SE on the $LiCoO_2$ particles formed a lithium-ion conducting path to the $LiCoO_2$ particles in the composite electrode. All-solid-state cells based on a combination of 10 wt.% SE particle mixing and SE (20 min) coating had a capacity of 95 mAh g^{-1}. The coating of a highly conductive SE on electrode particles is a promising technique to form an effective electrode–electrolyte interface and a lithium-ion conducting path in the composite, which should both contribute to the development of advanced all-solid-state lithium secondary batteries.

References

[1] J.-M. Tarascon, M. Armand, Nature 414 (2001) 359–367.
[2] H. Sakaebe, H. Matsumoto, Electrochem. Commun. 5 (2003) 594–598.
[3] H. Nakagawa, S. Izuchi, K. Kuwana, T. Nukuda, Y. Aihara, J. Electrochem. Soc. 150 (2003) A695–A700.
[4] B. Garcia, S. Lavallïee, G. Perron, C. Michot, M. Armand, Electrochem. Acta 49 (2004) 4583–4588.
[5] P.C. Howlett, D.R. MacFarlane, A.F. Hollenkamp, Electrochem. Solid-State Lett. 7 (2004) A97–A101.
[6] K. Zaghib, M. Simoneau, M. Armand, M. Gauthier, J. Power Sources 81–82 (1999) 300–305.
[7] S. Seki, Y. Kobayashi, H. Miyashiro, Y. Mita, T. Iwahori, Chem. Mater. 17 (2005) 2041–2045.
[8] R. Kanno, M. Murayama, T. Inada, T. Kobayashi, K. Sakamoto, N. Sonoyama, A. Yamada, S. Kondo, Electrochem. Solid-State Lett. 7 (2004) A455–A458.

[9] N. Ohta, K. Takada, L. Zhang, R. Ma, M. Osada, T. Sasaki, Adv. Mater. 18 (2006) 2226–2229.
[10] N. Ohta, K. Takada, I. Sakaguchi, L. Zhang, R. Ma, K. Fukuda, M. Osada, T. Sasaki, Electrochem. Commun. 9 (2007) 1486–1490.
[11] T. Kobayashi, A. Yamada, R. Kanno, Electrochim. Acta 53 (2008) 5045–5050.
[12] K. Takada, N. Aotani, K. Iwaomto, S. Kondo, Solid State Ionics 86–88 (1996) 877–882.
[13] N. Machida, H. Yamamoto, S. Asano, T. Shigematsu, Solid State Ionics 176 (2005) 473–479.
[14] F. Mizuno, S. Hama, A. Hayashi, K. Tadanaga, T. Minami, M. Tatsumisago, Chem. Lett. (2002) 1244–1245.
[15] A. Hayashi, T. Ohtomo, F. Mizuno, K. Tadanaga, M. Tatsumisago, Electrochem. Commun. 5 (2003) 701–705.
[16] Y. Seino, K. Takada, B.-C. Kim, L.-Q. Zhang, N. Ohta, H. Wada, M. Osada, T. Sasaki, Solid State Ionics 176 (2005) 2389–2393.
[17] T. Minami, A. Hayashi, M. Tatsumisago, Solid State Ionics 177 (2006) 2715–2720.
[18] A. Sakuda, A. Hayashi, M. Tatsumisago, Chem. Mater. 22 (2010) 949–956.
[19] R. Kanno, M. Murayama, J. Electrochem. Soc. 148 (2001) A742–A746.
[20] A. Hayashi, S. Hama, T. Minami, M. Tatsumisago, Electrochem. Commun. 5 (2003) 111–114.
[21] F. Mizuno, A. Hayashi, K. Tadanaga, M. Tatsumisago, Adv. Mater. 17 (2005) 918–921.
[22] A. Hayashi, S. Hama, F. Mizuno, K. Tadanaga, T. Minami, M. Tatsumisago, Solid State Ionics 175 (2004) 683–686.
[23] K. Takada, N. Ohta, L. Zhang, K. Fukuda, I. Sakaguchi, R. Ma, M. Osada, T. Sasaki, Solid State Ionics 179 (2008) 1333–1337.
[24] A. Sakuda, H. Kitaura, A. Hayashi, K. Tadanaga, M. Tatsumisago, Electrochem. Solid-State Lett. 11 (2008) A1–A3.
[25] A. Sakuda, H. Kitaura, A. Hayashi, K. Tadanaga, M. Tatsumisago, J. Electrochem. Soc. 156 (2009) A27–A32.
[26] A. Sakuda, H. Kitaura, A. Hayashi, K. Tadanaga, M. Tatsumisago, J. Power Sources 189 (2009) 527–530.
[27] F. Mizuno, A. Hayashi, K. Tadanaga, M. Tatsumisago, J. Power Sources 146 (2005) 711–714.
[28] A. Sakuda, A. Hayashi, T. Ohtomo, S. Hama, M. Tatsumisago, Electrochem. Solid-State Lett. 13 (2010) A73–A75.
[29] A. Sakuda, A. Hayashi, S. Hama, M. Tatsumisago, J. Am. Ceram. Soc. 93 (2010) 765–768.